Received: 20 February 2023 | Revised: 21 July 2023 | Accepted: 22 July 2023

DOI: 10.1111/sum.12952

Soil Use and Management | WILEY

RESEARCH PAPER

The use of visible and near-infrared spectroscopy for in-situ characterization of agricultural soil fertility: A proposition of best practice by comparing scanning positions and spectrometers

Konrad Metzger[1] | **Frank Liebisch**[2] | **Juan M. Herrera**[3] | **Thomas Guillaume**[1] | **Florian Walder**[4] | **Luca Bragazza**[1]

[1]Agroscope, Field-Crop Systems and Plant Nutrition, Nyon, Switzerland

[2]Agroscope, Water Protection and Substance Flows, Zurich, Switzerland

[3]Agroscope, Cultivation Techniques and Varieties in Arable Farming, Nyon, Switzerland

[4]Agroscope, Soil Quality and Soil Use, Zurich, Switzerland

Correspondence
Luca Bragazza, Agroscope, Field-Crop Systems and Plant Nutrition, Route de Duillier 50, P.O. Box 1012, CH-1260 Nyon, Switzerland.
Email: luca.bragazza@agroscope.admin.ch

Funding information
Agroscope; Horizon 2020 Framework Programme EJP Soil

Abstract

The application of visible and near-infrared (vis–NIR) spectroscopy to characterize soil samples has gained growing interest as a fast and cost-effective methodology for soil fertility assessment. In order to profit from the full potential of vis–NIR spectroscopy, the acquisition of soil spectra directly in-situ would increase the possibility to obtain data rapidly and at a high spatial and temporal resolution. In the present study, we test and propose the best practice to characterize a set of fertility-related parameters (i.e. texture, organic carbon, pH, cation exchange capacity and major nutrients) of agricultural soils by measuring vis–NIR spectra in the field. To reach this goal, we compare the spectra obtained from different scanning positions with two portable spectrometers, that is, a micro-electro-mechanical systems (MEMS)-based spectrometer and a research-grade vis–NIR spectrometer. On the basis of 134 soil sampling points, vis–NIR spectra were recorded from: (1) the cutaway side of a soil sample collected with an Edelman auger to a depth of 20 cm, (2) the raw soil surface, as well as (3) the cleaned and smoothed soil surface. Partial least squares regression (PLSR) calibration models were built for the selected soil parameters, scanning positions and different spectral pretreatments for both spectrometers. The model performance was evaluated based on the ratio of performance to interquartile range (RPIQ), the R^2, the root mean squared error (RMSE) and Lin's concordance correlation coefficient (CCC). Overall, the following soil parameters were successfully predicted: clay, sand, pH, organic carbon, cation exchange capacity, total nitrogen and exchangeable magnesium. In contrast, total and exchangeable Ca, K and P, as well as total Mg could not be predicted at a satisfactory level for both the spectrometers. The best scanning position for the successfully calibrated models was along the cutaway sides of the Edelman auger. Although the research-grade spectrometer gave better performance indicators for most of the parameters, the calibrations with

the MEMS-based spectrometer still resulted in satisfactory predictions. Based on these findings, the proposed best practice for obtaining in-situ soil vis–NIR scans is to scan along the cutaway sides of a soil core using at least five replicate scans.

KEYWORDS

best practice, MEMS spectrometer, soil fertility indicators, soil quality assessment, soil spectroscopy, vis–NIR spectroscopy

1 | INTRODUCTION

In the last decades, the use of visible and near-infrared (vis–NIR) spectroscopy for chemical and physical characterization of soil samples has gained a growing interest as a methodology for assessing soil fertility indicators (Demattê et al., 2022; Francos et al., 2022). More recently, the technical development of portable and affordable spectrometers has increased the interest for in-situ characterization of soil quality by vis–NIR spectroscopy (Fathy et al., 2020; Ng et al., 2020; Sharififar et al., 2019; Tang et al., 2020; Thomas et al., 2021).

Although the concept of soil fertility depends on the context in which it is used (Abbott & Johnson, 2017), multiple parameters have been suggested as soil fertility indicators for agricultural soils such as texture, pH, organic carbon (OC), cation exchange capacity (CEC) and major nutrient content (Bastida et al., 2008; Doran & Parkin, 1994; Gozukara et al., 2022; Karlen & Stott, 1994; Qi et al., 2009). The rationale of using spectroscopy is that spectra collected in the vis–NIR range (i.e. 350–2500 nm), as well as in the mid-infrared range (MIR, i.e. 2500–25,000 nm), can provide information about soil constituents (Dindaroglu et al., 2021; Soriano-Disla et al., 2014). Although the efficiency of vis–NIR spectroscopy to characterize soil fertility is still a matter of debate when compared with classical laboratory analyses, soil spectroscopy has anyway the potential to collect information at high spatial and temporal resolution, an opportunity particularly helpful for the implementation of precision agriculture technologies (Breure et al., 2022; Li et al., 2022; Semella et al., 2022).

The working principle of soil spectroscopy is the absorption of infrared light by chemical bonds of the molecules present in the soil constituents. In the vis–NIR range, the absorptions are mainly overtone and combination vibrations leading to broader peaks, whereas in the MIR range absorptions are mainly because of fundamental vibrations giving more details to the spectrum, but making the extraction of information more challenging (Stenberg et al., 2010; Viscarra Rossel et al., 2006). The main chemical bonds which react to vis–NIR radiation are C-H, C-N, O-H, C-O, C-N, N-O, C-C, Al-O, Fe-O and Si-O covalent bonds, all of which can be found in molecules associated with soil fertility (primary soil parameters) such as clay minerals, carbonates, iron-oxides and organic matter (Ben-Dor & Banin, 1995; Gozukara et al., 2021; Soriano-Disla et al., 2014; Stenberg et al., 2010). Calibration models for other secondary soil parameters such as micronutrients and trace elements have been trained by several authors but their predictive power is still a matter of debate (McBride, 2022; Viscarra Rossel et al., 2022).

The most common protocol for analysing soil samples by vis–NIR spectroscopy is to scan the samples after they have been air-dried and sieved to <2 mm or, additionally, finely ground (Bachion de Santana & Daly, 2022). With such a protocol, the samples are certainly uniform and well mixed with reduced influence from soil structure variability (e.g. voids, stones, bulk density) and, most importantly, from soil moisture, but still this protocol requires processing the soil samples in the laboratory. In order to profit from the full potential of vis–NIR spectroscopy, the acquisition of soil spectra directly on the field (in-situ) would be ideal to collect soil information at a high spatial and temporal resolution. The main challenge for this type of protocol lies in the in-situ characteristics of fresh soil, especially in relation to soil moisture, which has a strong influence on the spectra (Liu et al., 2022; Stenberg et al., 2010; Tang et al., 2020; Viscarra Rossel et al., 2009). Other potential errors associated with in-situ acquisition of spectra are related to losses of signal caused by a rough soil surface and to soil heterogeneities due, for example, to stones or plant residues (Ackerson et al., 2017; Ji et al., 2015).

Recently, mathematical methods have been developed to eliminate the influence of in-situ disturbances, such as (1) external parameter orthogonalization (EPO), where the undesired variability (introduced, e.g., by soil moisture) is analysed and removed from the spectra (Minasny et al., 2011; Roger et al., 2003), and (2) direct standardization (DS), where the discrepancy between laboratory and field spectra is calculated and removed from the dataset (Ji et al., 2015). These methodological developments, in combination with the development of compact and less expensive portable spectrometers, provide the potential to make use of vis–NIR spectroscopy directly in the field as an efficient and reliable method of soil fertility characterization.

The goal of our study is to test the in-situ vis–NIR spectroscopy as a tool to characterize the fertility of agricultural soils while assessing the best scanning methodology

directly in the field so to corroborate previous studies (Gras et al., 2014; Ji et al., 2016). More specifically, we want to provide a 'best practice' for obtaining reliable vis–NIR spectra in the field by answering the following research questions:

1. What is the best position to scan the soil in the field in order to obtain a good and robust predictive capacity of chemometric models tested for a set of 15 soil fertility-related parameters?
2. Do different classes of portable spectrometers (i.e. a compact MEMS (micro-electro-mechanical systems)-based spectrometer and a research-grade spectrophotometer) provide the same level of predictive quality for the investigated soil parameters?

2 | MATERIALS AND METHODS

2.1 | Sampling sites and soil laboratory analyses

A sampling campaign was conducted from spring to autumn 2021 in nine experimental fields of Agroscope, the Swiss competence center for agricultural research. The fields were situated at three Agroscope research sites across Switzerland: in Tänikon (Canton of Thurgau), in Reckenholz (Canton of Zurich) and in Changins (Canton of Vaud) (Figure 1). The experimental fields are composed of plots subjected to different agronomic treatments such as the amount and type of fertilizer application or the soil tillage intensity (Table 1). Within each experimental field, one soil sample was collected in each of the different treatment plots (= sampling point) with an Edelman auger (Eijkelkamp, NL) at a depth of 0–20 cm in the centre of the treatment plot ($n = 134$ soil samples). The total number of sampling points per experimental field was variable depending on the number of treatment plots.

Soil samples were stored in plastic bags in a cold room until they were dried at 40°C for 24 h and sieved to <2 mm for further analyses (Guillaume et al., 2021). Soil moisture content (105°C for 24 h) was immediately determined gravimetrically on a subsample of fresh soil. Using routine laboratory protocols (Table S2.1), the following physicochemical parameters were analysed: moisture, clay, sand, organic carbon (OC), total carbonates, cation exchange capacity

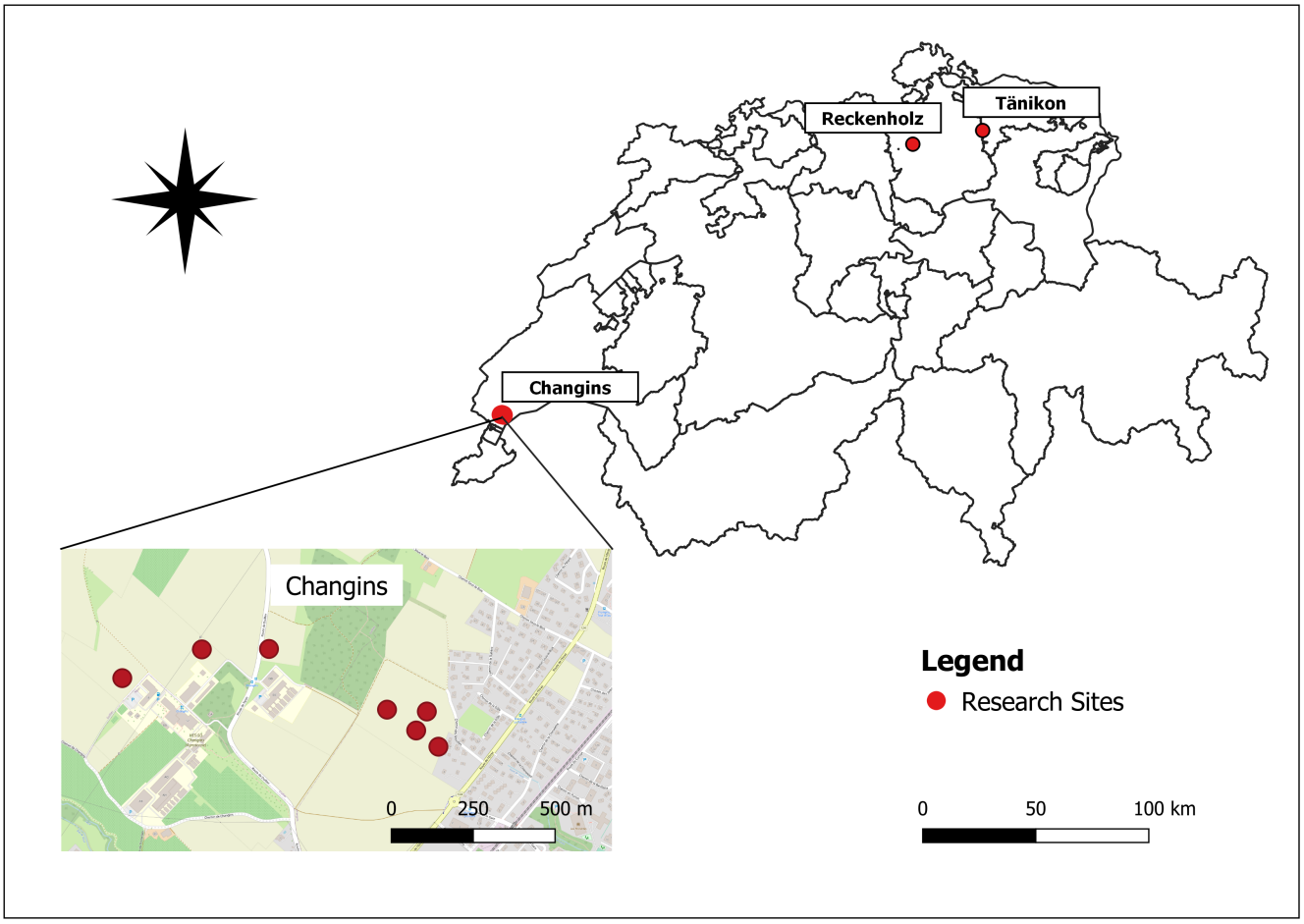

FIGURE 1 Location of the three Agroscope research sites within Switzerland. For the Changins site, the detailed location of the seven experimental fields is also reported.

TABLE 1 List of the research sites, code of the experimental fields and number of soil samples collected in each field. The crop indicates the species present at the time or just before the soil sampling, soil types are according to WRB.

Site name	Field code	Sampling points	Crop	Soil type
Tänikon	HB	12	Winter wheat, sowing	Cambisol/ Alisol
Reckenholz	ZOFE	24	Potato, harvested	Luvisol
Changins	11A	12	Winter wheat, harvested	Calcaric Cambisol
Changins	20	12	Corn, emerging	Calcaric Cambisol
Changins	24A	24	Oats, harvested	Calcaric Cambisol
Changins	29B	10	Corn, emerging	Calcaric Cambisol
Changins	29CA	12	Corn, emerging	Calcaric Cambisol
Changins	29CL	16	Corn, emerging	Calcaric Cambisol
Changins	29D	12	Corn, emerging	Calcaric Cambisol

TABLE 2 Technical characterization of the Spectral Evolution PSR + 3500 spectroradiometer (PSR) and the MEMS-based, handheld Fourier-transform (FT) NIR spectrometer NeoSpectra (NEO).

Instrument	PSR	NEO
Spectral range (nm)	350–2500	1350–2500
Spectral resolution (nm)	2.8 @ 700 nm 8 @ 1500 nm 6 @ 2100 nm	16
Spot size (mm)	10	10
Sample scanning	Contact probe with fibre optic and 5 W tungsten halogen light source	10 mm window with halogen light source
Detector	Si photodiode array (350–1000 nm) InGaAs photodiode array (970–1910 nm, 1900–2500 nm)	FT-NIR optical MEMS Michaelsen interferometer and InGaAs photodetector

(CEC), total nitrogen (N_tot), total phosphorus (P_tot), exchangeable phosphate (P_2O_5_OL), total potassium (K_tot), exchangeable potassium (K_2O_ex), total calcium (Ca_tot), exchangeable calcium (CaO_ex), total magnesium (Mg_tot) and exchangeable magnesium (MgO_ex).

2.2 | Spectrometers

Two spectrometers were used for the collection of soil spectra: the research-grade Spectral Evolution PSR + 3500 spectroradiometer ('PSR', Spectral Evolution), and a low-cost, MEMS-based, handheld Fourier-transform (FT) NIR spectrometer NeoSpectra Scanner ('NEO', Si-Ware Systems) (Table 2).

2.3 | Scanning positions of spectra in the field

Vis–NIR spectra were recorded at one position (= sampling point) per plot. First, a core was taken with the Edelman auger containing soil from 0 to 20 cm. Both the lateral soil surfaces of the extracted core were gently cut and straightened with a knife to guarantee good contact before being scanned at five points (serving as spectral replicates) per side with both the PSR and the NEO (hereafter called side_a and side_b) (Figure 2a). The soil was then extracted from the auger and stored in a plastic bag to be processed for laboratory analyses. For the *surface_raw* scans, the sensors were placed on the soil surface next to the auger hole after manually removing large plant residues or stones if present and the soil surface was scanned in five points as replicates (Figure 2b). For the *surface_smooth* scans, the previously scanned raw surface was smoothed by gently scratching across it with the shoe sole, breaking down the aggregates (so ensuring that good contact between the scanner and the soil was established) and the surface was scanned again in five points as replicates (Figure 2c). With the PSR spectrometer, the scans were recorded by means of a contact probe with an internal light source (5 W tungsten halogen) and auto-shutter, auto-exposure and auto-dark correction. The compact NEO spectrometer has an internal light source, the instrument was placed with the sapphire window directly on the soil, and scans were integrated over 5 s. At each sampling point, the spectrometers were calibrated with a white reference panel (i.e. every 25 scans). The five replicate scans

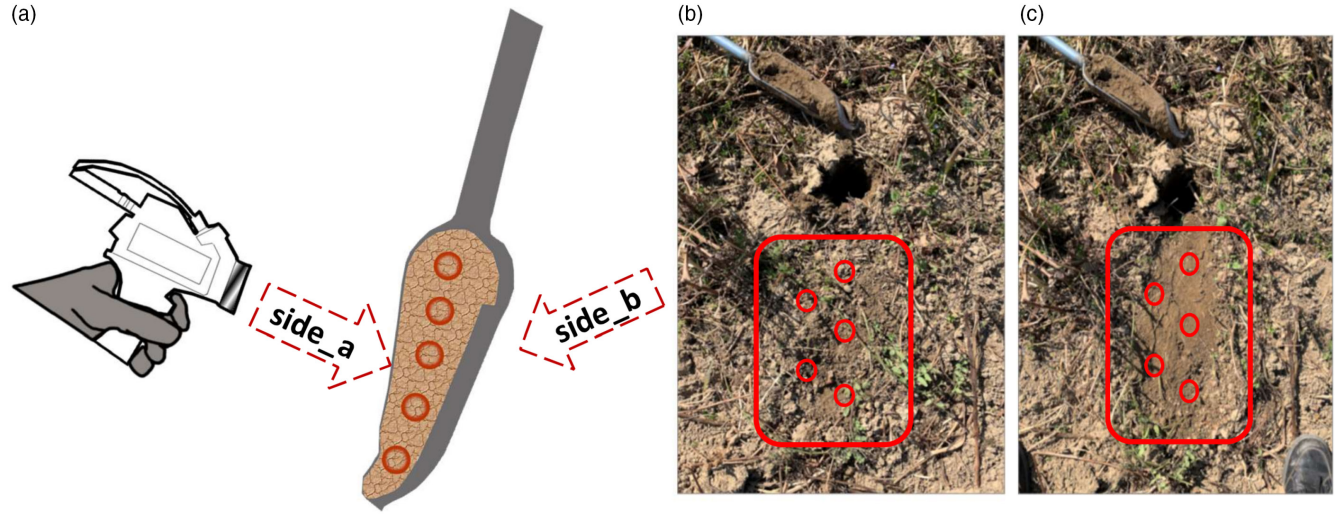

FIGURE 2 Schematic representation of the in-situ scanning protocol of soil samples with: (a) the scanning of the two sides of the Edelman auger (hereafter called side_a and side_b), (b) the scanning of the raw surface (surface_raw) and (c) the scanning of the cleaned and smoothed soil surface (surface_smooth).

at each position (side_a, side_b, surface_raw, surface_smooth) have been then averaged so to form one representative scan per scanning position and sampling point. In addition, the average of both cutaway soil sides of the auger ($n = 5 + 5$ replicates) was calculated so to assess the impact of increasing the number of replicates.

2.4 | Spectral processing

Data treatment was done using R 2022.02.3 (R Core Team, 2022) with the following packages: tidyverse (Wickham et al., 2019), prospectr (Stevens & Ramirez-Lopez, 2022), asdreader (Roudier, 2017) chemometrics (Filzmoser & Varmuza, 2011) and pls (Liland et al., 2021). The raw spectra for the PSR are reported in reflectance with a wavelength interval of 1 nm, whereas those of the NEO are reported with a ca. 13.5 cm^{-1} (wavenumber) resolution which corresponds to ca. 2.5–8.8 nm. To have a consistent wavelength interval, the NEO spectra were thus resampled to a 2 nm resolution and all spectra were transformed into absorbance ($A = 1/\log R$, with R being the measured reflectance). To check the stability of the five replicate scans, the spectral standard deviation (standard deviation across the replicates for each wavelength, then the standard deviation thereof along all wavelengths) was calculated (Metzger et al., 2020). When the spectral standard deviation was below the threshold of 0.01 all the spectra were accepted, if not, the scans were plotted and visually examined. If the spectra were only spread out but they followed the same pattern, they were left in the dataset, attributing the variability to the heterogeneity of the soil in the field. On the other hand, if some replicates were clearly not following the same pattern, we argued that this reading was not representative of the soil sample (e.g. because of specular reflection causing sensor errors) so the associated spectrum was removed from the dataset while the remaining replicates were used for averaging. Because of some sensor errors in the NEO, the data from 29 points could not be used and they have been removed from the dataset. In order to make the calibrations of the NEO and the PSR comparable, the same spectra were also removed from the PSR dataset, resulting in a total of 104 soil samples being effectively used. Some examples and a list of the removed spectra can be found in the supplementary material (SI 1 Outlier selection). After the data were cleaned, the resulting replicates of each scanning position (see Figure 2) were averaged to be used for future analyses. To minimize the influence of the soil moisture on the spectra, the regions known for H_2O absorptions, that is, 1350–1500 nm and 1850–2100 nm (Bowers & Hanks, 1965), were removed from both spectral datasets, as well as the region of 960–980 nm for the PSR in order to remove the irregularities resulting from the sensor transition (see Table 2). For the goals of this study, the spectra were not further processed to remove the influence of soil moisture (e.g. EPO or direct standardization). Mathematical pretreatment of the raw spectra is a common technique to enhance the information content of the raw spectra by smoothing, normalizing, removing scattering effects and enhancing the peaks through derivatization. The following mathematical pretreatments were applied to the raw spectra (RAW) so to enhance their information content: standard normal variate (SNV, [Barnes et al., 1989]), multiplicative scatter correction (MSC) (Geladi et al., 1985) and three different Savitzky–Golay (SG) smoothings and derivatives (Savitzky & Golay, 1964), all fitting a second-order polynomial (2) over 11 points (11): only smoothing

the spectra (no derivative, SG2110), smoothing and first derivative (SG2111) and smoothing and second derivative (SG2112). Together with the different scanning positions, this led to 24 (4 scanning positions×6 pretreatments) input datasets for each spectrometer.

2.5 | Modelling and model evaluation

Each of the input dataset was analysed by partial least squares regression (PLSR), an established technique to relate the spectra to laboratory analyses (Esbensen & Swarbrick, 2018). With PLSR, the number of variables (absorbance at each wavelength) is drastically reduced and the system is described by latent variables (LVs) for both the predictors (spectra) and the response variables (laboratory data) which are then used for multivariate regression. The model performance was evaluated through a repeated double cross-validation (rdCV) consisting of two nested cross-validations (CVs): the inner CV to optimize the number of LVs and the outer CV to evaluate the model performance. This procedure is then repeated 100 times, producing model performance indicators for each repetition. The inner CV is run as a 10-fold CV and the optimum number of LV is evaluated based on the standard error of prediction (SEP) of that loop with the 'hastie' method within the 'chemometrics' package for each iteration and then averaged and rounded over the four folds (Filzmoser et al., 2009; Filzmoser & Varmuza, 2011; Hutengs et al., 2019). The best combination of mathematical preprocessing and scanning position for each parameter was chosen based on the minimum SEP that was calculated after the 100 times rdCV. From the 100 repetitions, the average and standard deviation of the coefficient of determination (R^2), root mean squared error of the prediction (RMSEP), ratio of performance to interquartile range (RPIQ = IQR/RMSEP with IQR being the interquartile range (Q3 − Q1) of the laboratory parameter) and Lin's concordance correlation coefficient (CCC) as a measure of the agreement between predicted and laboratory data (Lin, 1989, 2000) were calculated.

3 | RESULTS

3.1 | Laboratory analyses and soil sample characterization

Our dataset covered a wide range of fertility-related parameters of Swiss agricultural soils. Some outliers were observed in the boxplots for clay because of high values in one experimental field (site 29CA where clay was >50%) and for OC probably because of organic residue remaining in the soil (Figure 3). On the other hand, the distribution of carbonates, total calcium, exchangeable potassium and magnesium showed a high number of outliers at high concentration values. The high values for carbonates and total calcium belong to the same research site (HB) characterized by high carbonate content soils. A complete

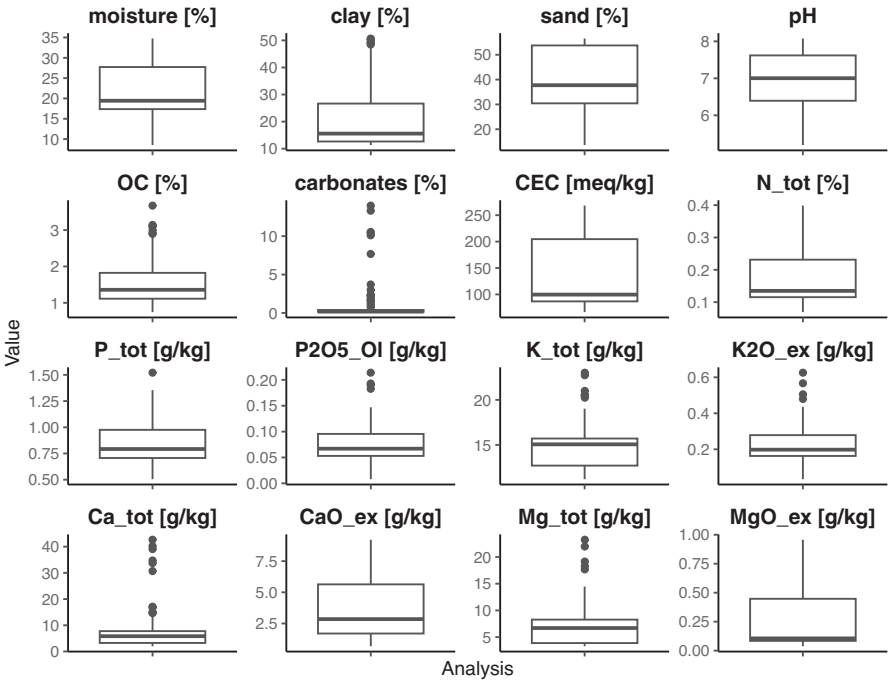

FIGURE 3 Boxplots of the analysed soil parameters showing the median (bold middle line), the upper and lower quartile (box) and the outliers (dots) for the examined soil parameters. Outliers are defined as values which are more than ±1.5×IQR (interquartile range) from the upper/lower quartile away. The summary statistics can be found in Table S2.1.

summary of the laboratory data can be found in the supplementary data (Table S2.1).

3.2 | Spectral shape and absorption features

Clear absorption features were visible around 1400 and 1900 nm for both instruments, as here reported for one representative sampling point (Figure 4). The overall reflectance was highest for the surface_smooth scanning positions. Conversely, the scans on both sides of the core (i.e. side_a and side_b) show the lowest reflectance values, whereas the surface_raw spectra showed a reflectance pattern intermediate between the smooth surface and the side positions. Another absorption feature can be seen around 2200 nm which was more detailed in the PSR than in the NEO.

The general shapes and main absorption features were very similar between the two spectrometers (Figure 4c). From the first absorption feature at 1400 nm, the NEO produced a steeper slope and ultimately a higher reflectance before the drop to the 1900 nm absorption feature. Over the entire spectrum, the reflectance of the NEO was shifted up to higher values, producing higher reflectance than the PSR scans.

3.3 | Spectral calibration results

For the PSR, the best predictions (based on the RPIQ) were for CEC (RPIQ 6.26 9 LVs, R^2 0.91, RMSEP 19.65 meq/kg), extractable MgO (RPIQ 4.4, 9 LVs, R^2 0.89, RMSEP 0.08 g/kg) and clay (RPIQ 3.69, 9 LVs, R^2 0.91, RMSEP 3.84%) (Table 3). The spectra pretreated with MSC and from the side_a (MgO_ex) or side_b (CEC and clay) scanning position provided the best results. For the NEO spectrometer, the best predictions were obtained also for CEC (RPIQ 5.55, 8 LVs, R^2 0.90, RMSEP 19.84 meq/kg), clay (RPIQ 4.73, 6 LVs, R^2 0.95, RMSEP 2.49%) and extractable magnesium (MgO_ex, RPIQ 2.95, 4 LVs, R^2 0.78, RMSEP 0.11 g/kg). The best combinations of scanning position and pretreatment were for CEC the SG2110 smoothed side_a spectra, for clay SG2110 and side_a and for MgO_ex first derivative (SG2111) and side_a. The wide range of laboratory values for the CEC (see Table S1) can explain the high RMSE, RMSEP and IQR values for both instruments (Table 3). The scatter plots of the laboratory values versus the predicted values for each physicochemical parameter can be found in the supplementary data (Figure S2.1-S2.4).

4 | DISCUSSION

4.1 | Spectral absorption features

For both instruments, there are clear absorption features around 1400 and 1900 nm because of water absorption, a result that is typical for vis–NIR spectra of soils because of stretching and bending of O-H and overtone and combination vibrations (Liu et al., 2022; Stenberg et al., 2010; Tang et al., 2020; Viscarra Rossel et al., 2009). In order to reduce the influence of soil moisture on the spectra, we

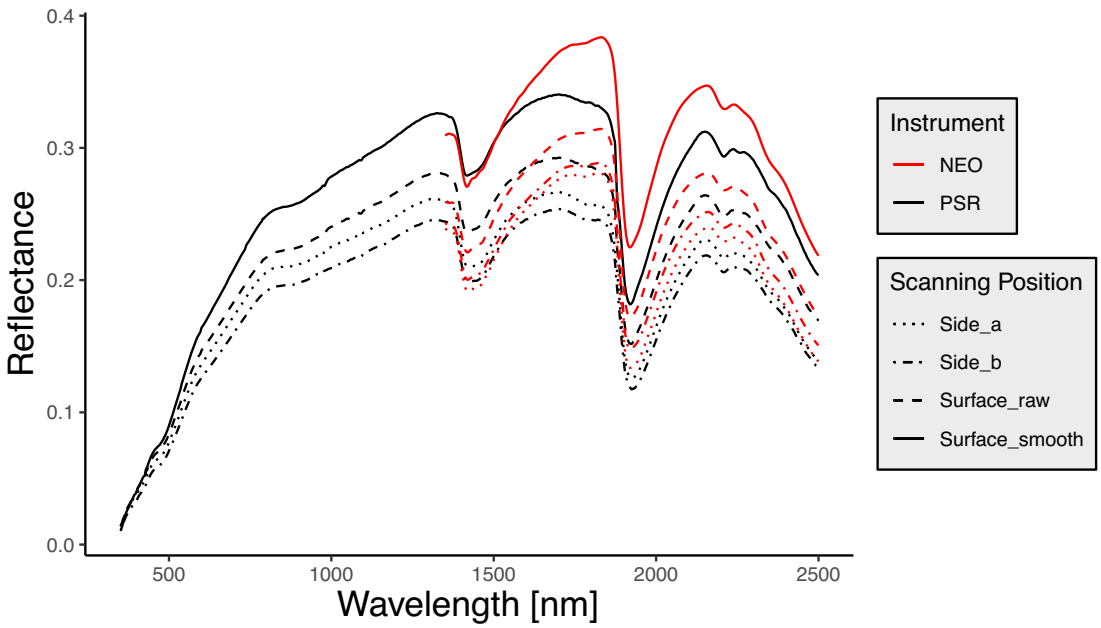

FIGURE 4 Reflectance spectra for the representative sampling point from the experimental field 20 for the PSR (black lines) and the NEO (red lines) and different sampling positions.

TABLE 3 The best scanning position, preprocessing method (RAW: unprocessed spectra, SNV: standard normal variate, MSC: multiplicative scatter correction, SG2110, SG2111,SG2112: Savitzky–Golay smoothing with 2nd polynomial over 11 points and no derivative, first derivative and second derivative), number of latent variables (LVs, rounded) for the two spectrometers (PSR and NEO) are reported in association with the model performance indicators: R^2, RMSE, RMSEP, IQR (interquartile range, Q3–Q1 of the laboratory values), RPIQ (ratio of performance to interquartile range = IQR/RMSEP) and bias. The numbers in brackets indicate the standard deviation.

Parameter	Scanning position	Preprocessing	LVs	R^2	RMSEP[a]	RPIQ	Lin's CCC	Bias	Ranking[b]
	PSR spectrometer								
CEC_[meq/kg]	side_b	MSC	9	0.91 (0.01)	19.65 (1.13)	6.26 (0.35)	0.95 (0.01)	−0.1 (0.83)	1
MgO_ex [g/kg]	side_a	MSC	9	0.89 (0.02)	0.08 (0.01)	4.4 (0.35)	0.93 (0.01)	0 (0)	2
clay [%]	side_b	MSC	9	0.91 (0.01)	3.84 (0.23)	3.69 (0.21)	0.95 (0.01)	−0.08 (0.14)	3
pH	side_b	MSC	9	0.74 (0.04)	0.39 (0.03)	3.34 (0.24)	0.85 (0.02)	0 (0.02)	4
OC [%]	side_b	MSC	5	0.71 (0.03)	0.37 (0.02)	3.19 (0.16)	0.84 (0.02)	0.01 (0.01)	5
sand [%]	side_a	SPC	9	0.88 (0.01)	3.96 (0.24)	3.06 (0.18)	0.94 (0.01)	0.03 (0.18)	6
N_tot [%]	side_b	MSC	4	0.86 (0.01)	0.05 (0)	2.91 (0.09)	0.81 (0.01)	0 (0)	7
CaO_ex [g/kg]	surface_smooth	SG2111	4	0.43 (0.06)	1.73 (0.09)	2.16 (0.12)	0.64 (0.04)	−0.01 (0.07)	8
Mg_tot [g/kg]	side_b	SNV	3	0.54 (0.07)	2.54 (0.18)	1.79 (0.12)	0.71 (0.05)	0.02 (0.09)	9
K_tot [g/kg]	side_a	SG2111	2	0.12 (0.02)	3.81 (0.05)	1.72 (0.02)	0.25 (0.02)	−0.01 (0.03)	10
P_tot [g/kg]	side_a	SG2110	2	0.35 (0.02)	0.18 (0)	1.25 (0.02)	0.36 (0.02)	0 (0)	11
P2O5_Ol [g/kg]	side_b	SNV	2	0.92 (0)	0.03 (0)	1.24 (0.03)	0.44 (0.03)	0 (0)	12
K2O_ex [g/kg]	side_b	SNV	2	0.52 (0.01)	0.1 (0)	0.92 (0.01)	0.28 (0.02)	0 (0)	13
Ca_tot [g/kg]	side_b	SNV	3	0.26 (0.09)	6.72 (0.42)	0.52 (0.03)	0.45 (0.09)	0.09 (0.24)	14
carb [%]	side_b	SNV	3	0.16 (0.07)	2.4 (0.1)	0.13 (0.01)	0.34 (0.06)	0.04 (0.07)	15
	NEO spectrometer								
CEC [meq/kg]	side_a	SG2110	8	0.9 (0.01)	19.84 (1.22)	5.55 (0.34)	0.95 (0.01)	−0.58 (1.82)	1
MgO_ex [g/kg]	side_a	SG2111	4	0.78 (0.04)	0.11 (0.01)	2.95 (0.27)	0.85 (0.03)	0.003 (0.01)	3
clay [%]	side_a	SG2110	6	0.95 (0)	2.94 (0.13)	4.73 (0.21)	0.97 (0)	−0.29 (0.32)	2
pH	surface_smooth	SG2111	4	0.42 (0.08)	0.58 (0.04)	2.16 (0.14)	0.62 (0.06)	−0.002 (0.03)	8
OC [%]	side_a	SG2111	3	0.64 (0.02)	0.41 (0.01)	2.72 (0.07)	0.78 (0.01)	0.001 (0.01)	6
sand [%]	side_a	SG2110	4	0.86 (0.02)	4.44 (0.24)	2.94 (0.14)	0.93 (0.01)	0.01 (0.16)	4
N_tot [%]	side_a	SG2111	2	0.87 (0.01)	0.05 (0)	2.92 (0.1)	0.81 (0.02)	0.00 (0.001)	5
CaO_ex [g/kg]	side_a	SG2110	8	0.43 (0.08)	1.7 (0.12)	2.23 (0.16)	0.67 (0.05)	−0.01 (0.03)	7
Mg_tot [g/kg]	side_a	MSC	2	0.4 (0.04)	2.57 (0.1)	1.78 (0.07)	0.59 (0.04)	0.002 (0.07)	9
K_tot [g/kg]	surface_smooth	SPC	6	0.05 (0.08)	4.06 (0.18)	1.75 (0.08)	0.25 (0.1)	−0.01 (0.04)	10
P_tot [g/kg]	side_a	SG2111	2	0.31 (0.03)	0.18 (0)	1.12 (0.02)	0.23 (0.03)	0.00 (0.003)	11
P2O5_Ol [g/kg]	side_a	SG2111	2	0.9 (0)	0.03 (0)	0.96 (0.02)	0.09 (0.03)	0.00 (0.001)	12
K2O_ex [g/kg]	side_b	SG2112	2	0.56 (0.01)	0.1 (0)	0.82 (0.01)	0.29 (0.02)	0.00 (0.001)	13
Ca_tot [g/kg]	surface_smooth	SG2110	2	0.13 (0.02)	5.34 (0.06)	0.63 (0.01)	0.27 (0.02)	−0.02 (0.04)	14
Carbonates [%]	Surface_smooth	SPC	2	0.01 (0.02)	1.62 (0.02)	0.16 (0)	0.07 (0.02)	−0.01 (0.02)	15

[a]Units of RMSEP and bias are the same as its corresponding parameter.

[b]Ranked by descending RPIQ on the basis of the results from the PSR models.

removed the areas corresponding to these wavelengths. Another absorption feature because of O-H stretching and metal-O-H bending can be seen around 2200 nm (Viscarra Rossel et al., 2009), particularly in the PSR because of the higher spectral resolution compared with the NEO.

The overall reflectance is higher for the surface_ smooth scanning positions because a smooth soil surface can reflect a greater fraction of the incoming radiation and because the soil surface dries faster than the cutaways soil sides in the core (Gras et al., 2014; Viscarra Rossel et al., 2009). Over the entire spectrum, the reflectance of the NEO is shifted up to higher values so producing higher reflectance than the PSR scans. This shift has been reported also by other studies (Gorla et al., 2022) and is likely because of intrinsic instrument properties.

4.2 | Spectral calibration

Based on a threshold of RPIQ >1.89 and Lins's CC, the analysis of the model performance parameters shows that out of the 15 soil physicochemical parameters, for seven of them a satisfactory model can be calibrated with the PSR data. The RPIQ threshold of 1.89, as proposed by Ludwig et al. (2019) and based on Chang et al. (2001), is currently used to distinguish satisfactory from unsatisfactory calibrations (Francos et al., 2022; Greenberg et al., 2020; Leenen et al., 2022). However, it should be kept in mind that these thresholds are arbitrary and must be defined in the context of the specific research questions (Bellon-Maurel et al., 2010; Reeves & Smith, 2009). Based on the above threshold in combination with Lin's CCC, the RMSEP and the R^2, our study indicates that a satisfactory prediction can be obtained for the following soil parameters: CEC, clay, sand, pH, MgO_ex, OC, N_tot, well in accordance with previous studies (Barra et al., 2021; Soriano-Disla et al., 2014). For CaO_ex and Mg_tot, the RPIQ is >1.89 but the values of Lin's CC (<0.8) and R^2 (<0.66) indicate unsatisfactory calibration. The other parameters that could not satisfactorily be calibrated are total and extractable K, total and extractable P, total Ca and carbonates in line with the results of previous studies (McBride, 2022; Viscarra Rossel et al., 2006). Although in other studies the carbonates were well calibrated (see Barra et al. (2021), the unsatisfactory performance in our study is probably related to the high number of outliers, similarly to Ca_tot concentration (see Figure 3).

For the NEO spectrometer, satisfactory models could be built for six parameters. The parameters are the same as for the PSR, with the exception of pH, which has a RPIQ of 2.16, but the Lin's CCC (0.62) and the R^2 (0.42) suggest an insufficient model performance.

4.3 | In-situ scanning position and proposed best practice

Based on the scanning positions leading to the best model results for the PSR, we can observe as all the soil parameters with satisfactory models (i.e. RPIQ >1.89 show a better performance with scans taken from the cutaway sides.

For the NEO spectrometer (Table 3), satisfactory models with RPIQ >1.89 were obtained for six soil parameters with scans taken from the cutaway sides of the soil core.

Based on the model results, scanning along one side of the soil core seems the best scanning position and practice. This practice also offers the most plausible and useful results considering that most of the laboratory analyses

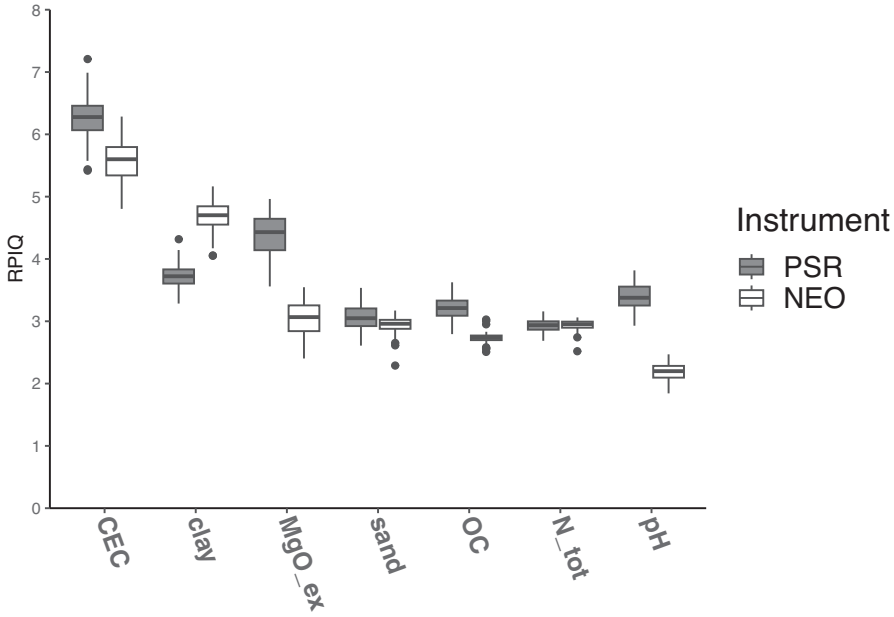

FIGURE 5 Boxplots of the RPIQ (IQR/RMSEP) values of the PSR (full) and the NEO (empty) for the best scanning position (see Table 3).

are performed on samples taken at this depth. In addition, we must consider that because the soil surface is exposed to external inputs (sun, rain, plant residues) the predicted values from this position might divert considerably from the bulk sample. Thus, scanning the soil along the side of a soil core is the preferred position for in field spectra acquisition. This finding corroborates previous studies (Gras et al., 2014; Ji et al., 2016) in which the scanning of the soil along the core sides appeared as the best field protocol using a full-range spectrometer.

Our data show that increasing the number of replicate scans on both the sides of the soil core (i.e. the average of side_a plus side_b, $n=10$) do not improve the performances of the models for the successfully predicted parameters. This result is consistent with the expected similarity of the two cutaways of the soil core and, in addition, it allows to reduce the time of the scan acquisition by focusing on only one cutaway side.

4.4 | Comparison of PSR and NEO based on the proposed best practice protocol

The RPIQ from the 100 times repeated rdCV of the seven successfully calibrated parameters for the PSR and the NEO are shown in Figure 5. When the performances of the two instruments are compared (Table 3), the PSR usually performs better in terms of RPIQ, but, unexpectedly, for clay, the RPIQ for the NEO was higher because of the decreased RMSEP (3.48% for PSR and 2.94% for the NEO, respectively).The reason for that remains unclear, but it could be because of the fact that important clay-associated absorptions are found in the range in which the NEO operates (1350–2500 nm) (Viscarra Rossel & Behrens, 2010), so that the visible region covered by the PSR only contributes as noise. However, for both PSR and NEO, the RMSEP values are within the range (2.9–4%) found by other authors (Viscarra Rossel et al., 2006). Overall, the results exhibit a very low bias, especially for the PSR (<0.1), while the NEO showed higher biases for CEC (−0.58) and clay (−0.29). This bias might be caused by the reduced range of the NEO compared with the PSR, even if further examinations are necessary to confirm this hypothesis.

The high RPIQ values of CEC can probably be explained by the strong correlation of CEC with OC (Pearson $r^2=0.81$, $n=134$) and clay (Pearson $r^2=0.89$, $n=134$) and the wide range of CEC in the laboratory values (70–289 meq/kg). Even if the OC does not show such a high RPIQ compared with the other parameters, the RMSEP of 0.37% and 0.41% for both the PSR and the NEO are within the range of other publications (Hutengs et al., 2019; Viscarra Rossel et al., 2006).

The NEO spectrometer became available recently, and several authors have used it or other MEMS-based spectrometers in the context of soil analysis for OC, texture, pH and nutrient analysis as well as in comparative studies with research-grade spectrometers (Angeletti da Fonseca et al., 2022; Goodwin et al., 2022; Karyotis et al., 2021; Ng et al., 2020; Pasquini & Hespanhol, 2021; Sharififar et al., 2019; Tang et al., 2020; Thomas et al., 2021). Overall, it appears that the NEO spectrometer, as other low-cost MEMS instruments, are less performing than the full-range spectrometers, but that they show a potential for future applications (Karyotis et al., 2021; Tang et al., 2020; Thomas et al., 2021).

Using the NEO spectrometer in comparative studies with research-grade spectrometers (PSR, ASD), other authors have found generally better performances of the research-grade instruments, but comparable results for some parameters (e.g. texture, pH, carbon) from dried and ground samples (Tang et al., 2020; Thomas et al., 2021). Ng et al. (2020) started to build a spectral library with spectra collected with the NEO spectrometer for several soil parameters (including texture, carbon, pH and nutrients) and they used the predicted results to calculate fertilizer application recommendations. In a different approach to soil sampling, Angeletti da Fonseca et al. (2022) used the NEO spectrometer in combination with a sampling device where the dried and ground soil was scanned in a rotating bottle to increase the scanned surface (Pasquini & Hespanhol, 2021) so improving the prediction of soil OC considerably.

We underline that the influence and the correction of field moisture have not been taken into consideration for this study because this topic will be specifically addressed in future studies with additional experiments and sampling, once the best practice of in-situ soil scanning has been clarified. This will be one of the challenges for future routine in-situ analysis of soil fertility with vis–NIR spectroscopy, among other challenges such as the selection of a representative calibration set, the construction of a spectral library or the development of a transfer function between in-situ spectra and an existing spectral library. Another challenge will be to determine the precision and accuracy of the predicted measurements by different types of vis–NIR spectrometers for agricultural decision support, especially if many soil indicators are considered and evaluated in classes instead of using continuous values (Flisch et al., 2017; Sinaj et al., 2017; Wall & Plunkett, 2016).

5 | CONCLUSIONS

Our study has clearly demonstrated the feasibility of using portable vis–NIR spectrometers to measure,

in-situ, a set of soil fertility indicators such as clay, OC, N_tot, pH and CEC. We have found that, in the field, the best scanning position for soil samples is along cutaway sides of a 20 cm long core where the PLSR models can be calibrated successfully (RPIQ >1.89). By comparing two different instruments, we showed that the PSR spectrometer performed better than the NEO spectrometer (higher RPIQ). However, it was still possible to successfully calibrate the cheaper NEO spectrometer for the same soil parameters as the PSR spectrometer, with the only exception of pH.

ACKNOWLEDGEMENTS

This study is part of the research project '*A simple way to measure soil fertility*' which is funded by the Agroscope Research Programme *'Indicate - Measuring and Optimising Farm Environmental Impacts'*. This study was co-funded by the Horizon 2020 European Joint Program (EJP) SOIL project '*ProbeField*'. The authors are grateful to Saïd Elfouki, Yves Grosjean, Francesco Argento, Cecil Ringger, Simon Treier, Nicolas Vuille-dit-Bille and Hansueli Zbinden for their help during field sampling and sample processing. We acknowledge the helpful advice from Michael Simmler (Agroscope Tänikon) for modelling and programming, as well as his help during fieldwork. Open access funding provided by Agroscope.

DATA AVAILABILITY STATEMENT

The data that support the findings of this study are available from the corresponding author upon reasonable request.

ORCID

Konrad Metzger https://orcid.org/0000-0002-8075-0252
Frank Liebisch https://orcid.org/0000-0003-0000-7491
Juan M. Herrera https://orcid.org/0000-0002-9398-7224
Thomas Guillaume https://orcid.org/0000-0002-6926-9337
Luca Bragazza https://orcid.org/0000-0001-8583-284X

REFERENCES

Abbott, L. K., & Johnson, N. C. (2017). *Introduction: Perspectives on mycorrhizas and soil fertility*. Fertility, Structure, and Carbon Storage. Elsevier Inc. https://doi.org/10.1016/B978-0-12-804312-7.00006-1

Ackerson, J. P., Morgan, C. L. S., & Ge, Y. (2017). Penetrometer-mounted VisNIR spectroscopy: Application of EPO-PLS to in situ VisNIR spectra. *Geoderma*, *286*, 131–138. https://doi.org/10.1016/j.geoderma.2016.10.018

Angeletti da Fonseca, A., Pasquini, C., Cristina Costa, D., & Barros Soares, E. M. (2022). Effect of the sample measurement representativeness on soil carbon determination using near-infrared compact spectrophotometers. *Geoderma*, *409*, 115636. https://doi.org/10.1016/j.geoderma.2021.115636

Bachion de Santana, F., & Daly, K. (2022). A comparative study of MIR and NIR spectral models using ball-milled and sieved soil for the prediction of a range soil physical and chemical parameters. *Spectrochim. Acta Part A Mol. Biomol. Spectrosc.*, *279*, 121441. https://doi.org/10.1016/j.saa.2022.121441

Barnes, R. J., Dhanoa, M. S., & Lister, S. J. (1989). Standard normal variate transformation and de-trending of near-infrared diffuse reflectance spectra. *Applied Spectroscopy*, *43*, 772–777. https://doi.org/10.1366/0003702894202201

Barra, I., Haefele, S. M., Sakrabani, R., & Kebede, F. (2021). Soil spectroscopy with the use of chemometrics, machine learning and pre-processing techniques in soil diagnosis: Recent advances–a review. *TrAC - Trends Anal. Chem.*, *135*, 116166. https://doi.org/10.1016/j.trac.2020.116166

Bastida, F., Zsolnay, A., Hernández, T., & García, C. (2008). Past, present and future of soil quality indices: A biological perspective. *Geoderma*, *147*, 159–171. https://doi.org/10.1016/j.geoderma.2008.08.007

Bellon-Maurel, V., Fernandez-Ahumada, E., Palagos, B., Roger, J. M., & McBratney, A. (2010). Critical review of chemometric indicators commonly used for assessing the quality of the prediction of soil attributes by NIR spectroscopy. *TrAC - Trends Anal. Chem.*, *29*, 1073–1081. https://doi.org/10.1016/j.trac.2010.05.006

Ben-Dor, E., & Banin, A. (1995). Near-infrared analysis as a rapid method to simultaneously evaluate several soil properties. *Soil Science Society of America Journal*, *59*, 364–372. https://doi.org/10.2136/sssaj1995.03615995005900020014x

Bowers, S. A., & Hanks, R. J. (1965). Reflection of radiant energy from soils. *Soil Science*, *100*, 130–138. https://doi.org/10.1097/00010694-196508000-00009

Breure, T. S., Haefele, S. M., Hannam, J. A., Corstanje, R., Webster, R., Moreno-Rojas, S., & Milne, A. E. (2022). A loss function to evaluate agricultural decision-making under uncertainty: A case study of soil spectroscopy. *Precision Agriculture*, *23*, 1333–1353. https://doi.org/10.1007/s11119-022-09887-2

Chang, C.-W., Laird, D. A., Mausbach, M. J., & Hurburgh, C. R. (2001). Near-infrared reflectance spectroscopy–principal components regression analyses of soil properties. *Soil Science Society of America Journal*, *65*, 480–490. https://doi.org/10.2136/sssaj2001.652480x

Demattê, J. A. M., da Paiva, A. F., Poppiel, R. R., Rosin, N. A., Ruiz, L. F. C., de Mello, F. A., Minasny, B., Grunwald, S., Ge, Y., Ben Dor, E., Gholizadeh, A., Gomez, C., Chabrillat, S., Francos, N., Ayoubi, S., Fiantis, D., Biney, J. K. M., Wang, C., Belal, A., … Silvero, N. E. Q. (2022). The Brazilian soil spectral service (BraSpecS): A user-friendly system for global soil spectra communication. *Remote Sensing*, *14*, Article 740. https://doi.org/10.3390/rs14030740

Dindaroglu, T., Babur, E., Yakupoglu, T., Rodrigo-Comino, J., & Cerdà, A. (2021). Evaluation of geomorphometric characteristics and soil properties after a wildfire using Sentinel-2 MSI imagery for future fire-safe forest. *Fire Safety Journal*, *122*, 103318. https://doi.org/10.1016/j.firesaf.2021.103318

Doran, J. W., & Parkin, T. B. (1994). Defining and assessing soil quality. *SSSA Spec. Publ.*, *35*, 1–21.

Esbensen, K. H., & Swarbrick, B. (2018). *Multivariate Data Analysis* (6th ed.). Camo Software AS.

Fathy, A., Sabry, Y. M., Nazeer, S., Bourouina, T., & Khalil, D. A. (2020). On-chip parallel Fourier transform spectrometer for broadband selective infrared spectral sensing. *Microsystems & Nanoengineering*, *6*, Article 10. https://doi.org/10.1038/s41378-019-0111-0

Filzmoser, P., Liebmann, B., & Varmuza, K. (2009). Repeated double cross validation. *Journal of Chemometrics*, *23*, 160–171. https://doi.org/10.1002/cem.1225

Filzmoser, P., & Varmuza, K. (2011). Chemometrics: multivariate statistical analysis in chemometrics.

Flisch, R., Neuweiler, R., Kuster, T., Oberholzer, H., Hugueneni-Elie, O., & Richner, W. (2017). Bodeneigenschaften und Bodenanalysen. *Agrarforschung Schweiz*, *8*(6), 2/1–2/34 [Spezialpublikation].

Francos, N., Gholizadeh, A., Demattê, J. A. M., & Ben-Dor, E. (2022). Effect of the internal soil standard on the spectral assessment of clay content. *Geoderma*, *420*, 115873. https://doi.org/10.1016/j.geoderma.2022.115873

Geladi, P., MacDougall, D., & Martens, H. (1985). Linearization and scatter-correction for near-infrared reflectance spectra of meat. *Applied Spectroscopy*, *39*, 491–500. https://doi.org/10.1366/0003702854248656

Goodwin, D. J., Kane, D. A., Dhakal, K., Covey, K. R., Bettigole, C., Hanle, J., Ortega, S., Perotto-Baldivieso, H. L., Fox, W. E., & Tolleson, D. R. (2022). Can low-cost, handheld spectroscopy tools coupled with remote sensing accurately estimate soil organic carbon in semi-arid grazing lands? *Soil Systems*, *6*, Article 38. https://doi.org/10.3390/soilsystems6020038

Gorla, G., Taiana, A., Boqu, R., Bani, P., Gachiuta, O., & Giussani, B. (2022). Unravelling error sources in miniaturized NIR spectroscopic measurements: The case study of forages. *Analytica Chimica Acta*, *1211*, 339900. https://doi.org/10.1016/j.aca.2022.339900

Gozukara, G., Acar, M., Ozlu, E., Dengiz, O., Hartemink, A. E., & Zhang, Y. (2022). A soil quality index using Vis-NIR and pXRF spectra of a soil profile. *Catena*, *211*, 105954. https://doi.org/10.1016/j.catena.2021.105954

Gozukara, G., Zhang, Y., & Hartemink, A. E. (2021). Using Vis-NIR and pXRF data to distinguish soil parent materials – An example using 136 pedons from Wisconsin, USA. *Geoderma*, *396*, 115091. https://doi.org/10.1016/j.geoderma.2021.115091

Gras, J. P., Barthès, B. G., Mahaut, B., & Trupin, S. (2014). Best practices for obtaining and processing field visible and near infrared (VNIR) spectra of topsoils. *Geoderma*, *214–215*, 126–134. https://doi.org/10.1016/j.geoderma.2013.09.021

Greenberg, I., Linsler, D., Vohland, M., & Ludwig, B. (2020). Robustness of visible near-infrared and mid-infrared spectroscopic models to changes in the quantity and quality of crop residues in soil. *Soil Science Society of America Journal*, *84*, 963–977. https://doi.org/10.1002/saj2.20067

Guillaume, T., Bragazza, L., Levasseur, C., Libohova, Z., & Sinaj, S. (2021). Long-term soil organic carbon dynamics in temperate cropland-grassland systems. *Agriculture, Ecosystems and Environment*, *305*, 107184. https://doi.org/10.1016/j.agee.2020.107184

Hutengs, C., Seidel, M., Oertel, F., Ludwig, B., & Vohland, M. (2019). In situ and laboratory soil spectroscopy with portable visible-to-near-infrared and mid-infrared instruments for the assessment of organic carbon in soils. *Geoderma*, *355*, 113900. https://doi.org/10.1016/j.geoderma.2019.113900

Ji, W., Li, S., Chen, S., Shi, Z., Viscarra Rossel, R. A., & Mouazen, A. M. (2016). Prediction of soil attributes using the Chinese soil spectral library and standardized spectra recorded at field conditions. *Soil and Tillage Research*, *155*, 492–500. https://doi.org/10.1016/j.still.2015.06.004

Ji, W., Viscarra Rossel, R. A., & Shi, Z. (2015). Accounting for the effects of water and the environment on proximally sensed Vis-NIR soil spectra and their calibrations. *European Journal of Soil Science*, *66*, 555–565. https://doi.org/10.1111/ejss.12239

Karlen, D. L., & Stott, D. E. (1994). A framework for evaluating physical and chemical indicators of soil quality. Defin. Soil Qual. a sustain. Environ. Proc. *Symp. Minneapolis, MN*, *1992*, 53–72. https://doi.org/10.2136/sssaspecpub35.c4

Karyotis, K., Angelopoulou, T., Tziolas, N., Palaiologou, E., Samarinas, N., & Zalidis, G. (2021). Evaluation of a micro-electro mechanical systems spectral sensor for soil properties estimation. *Land*, *10*, 1–16. https://doi.org/10.3390/land10010063

Leenen, M., Pätzold, S., Tóth, G., & Welp, G. (2022). A LUCAS-based mid-infrared soil spectral library: Its usefulness for soil survey and precision agriculture. *Journal of Plant Nutrition and Soil Science*, *185*, 370–383. https://doi.org/10.1002/jpln.202100031

Li, S., Viscarra Rossel, R. A., & Webster, R. (2022). The cost-effectiveness of reflectance spectroscopy for estimating soil organic carbon. *European Journal of Soil Science*, *73*(1), e13202. https://doi.org/10.1111/ejss.13202

Liland, K. H., Mevik, B.-H., Wehrens, R., 2021. Pls: Partial least squares and principal component regression.

Lin, L. I.-K. (1989). A concordance correlation coefficient to evaluate reproducibility. *Biometrics*, *45*, 255. https://doi.org/10.2307/2532051

Lin, L. I.-K. (2000). A note on the concordance correlation coefficient. *Biometrics*, *56*, 324–325. https://doi.org/10.1111/j.0006-341X.2000.00324.x

Liu, J., Zhang, D., Yang, L., Ma, Y., Cui, T., He, X., & Du, Z. (2022). Developing a generalized Vis-NIR prediction model of soil moisture content using external parameter orthogonalization to reduce the effect of soil type. *Geoderma*, *419*, 115877. https://doi.org/10.1016/j.geoderma.2022.115877

Ludwig, B., Murugan, R., Parama, V. R. R., & Vohland, M. (2019). Accuracy of estimating soil properties with mid-infrared spectroscopy: Implications of different Chemometric approaches and software packages related to calibration sample size. *Soil Science Society of America Journal*, *83*, 1542–1552. https://doi.org/10.2136/sssaj2018.11.0413

McBride, M. B. (2022). Estimating soil chemical properties by diffuse reflectance spectroscopy: Promise versus reality. *European Journal of Soil Science*, *73*, 1–11. https://doi.org/10.1111/ejss.13192

Metzger, K., Zhang, C., Ward, M., & Daly, K. (2020). Mid-infrared spectroscopy as an alternative to laboratory extraction for the determination of lime requirement in tillage soils. *Geoderma*, *364*, 114171. https://doi.org/10.1016/j.geoderma.2020.114171

Minasny, B., McBratney, A. B., Bellon-Maurel, V., Roger, J. M., Gobrecht, A., Ferrand, L., & Joalland, S. (2011). Removing the effect of soil moisture from NIR diffuse reflectance spectra for the prediction of soil organic carbon. *Geoderma*, *167–168*, 118–124. https://doi.org/10.1016/j.geoderma.2011.09.008

Ng, W., Husnain, A., Siregar, A. F., Hartatik, W., Sulaeman, Y., Jones, E., & Minasny, B. (2020). Developing a soil spectral library using a low-cost NIR spectrometer for precision fertilization in Indonesia. *Geoderma Regional*, *22*, e00319. https://doi.org/10.1016/j.geodrs.2020.e00319

Pasquini, C., & Hespanhol, M. C. (2021). A rotational-linear sample probing device to improve the performance of compact near-infrared spectrophotometers. *Microchemical Journal*, *170*, 106747. https://doi.org/10.1016/j.microc.2021.106747

Qi, Y., Darilek, J. L., Huang, B., Zhao, Y., Sun, W., & Gu, Z. (2009). Evaluating soil quality indices in an agricultural region of Jiangsu Province, China. *Geoderma*, *149*, 325–334. https://doi.org/10.1016/j.geoderma.2008.12.015

R Core Team. (2022). *R: A language and environment for statistical computing*. R Found. Stat.

Reeves, J. B., & Smith, D. B. (2009). The potential of mid- and near-infrared diffuse reflectance spectroscopy for determining major- and trace-element concentrations in soils from a geochemical survey of North America. *Applied Geochemistry*, *24*, 1472–1481. https://doi.org/10.1016/j.apgeochem.2009.04.017

Roger, J. M., Chauchard, F., & Bellon-Maurel, V. (2003). EPO-PLS external parameter orthogonalisation of PLS application to temperature-independent measurement of sugar content of intact fruits. *Chemometrics and Intelligent Laboratory Systems*, *66*, 191–204. https://doi.org/10.1016/S0169-7439(03)00051-0

Roudier, P., 2017. Asdreader: Reading ASD binary files in R.

Savitzky, A., & Golay, M. J. E. (1964). Smoothing and differentiation of data by simplified least squares procedures. *Analytical Chemistry*, *36*, 1627–1639. https://doi.org/10.1021/ac60214a047

Semella, S., Hutengs, C., Seidel, M., Ulrich, M., Schneider, B., Ortner, M., Thiele-Bruhn, S., Ludwig, B., & Vohland, M. (2022). Accuracy and reproducibility of laboratory diffuse reflectance measurements with portable VNIR and MIR spectrometers for predictive soil organic carbon modeling. *Sensors*, *22*, 2749. https://doi.org/10.3390/s22072749

Sharififar, A., Singh, K., Jones, E., Ginting, F. I., & Minasny, B. (2019). Evaluating a low-cost portable NIR spectrometer for the prediction of soil organic and total carbon using different calibration models. *Soil Use and Management*, *35*, 607–616. https://doi.org/10.1111/sum.12537

Sinaj, S., Charles, R., Baux, A., Dupuis, B., Hiltbrunner, J., Levy, L., Pellet, D., Blanchet, G., & Jeangros, B. (2017). 8/Düngung von Ackerkulturen. *Agrar. Schweiz*, *8*, 163–165.

Soriano-Disla, J. M., Janik, L. J., Viscarra Rossel, R. A., MacDonald, L. M., & McLaughlin, M. J. (2014). The performance of visible, near-, and mid-infrared reflectance spectroscopy for prediction of soil physical, chemical, and biological properties. *Applied Spectroscopy Reviews*, *49*, 139–186. https://doi.org/10.1080/05704928.2013.811081

Stenberg, B., Viscarra Rossel, R. A., Mouazen, A. M., & Wetterlind, J. (2010). Visible and near infrared spectroscopy in soil science. *Advances in Agronomy*, *107*, 163–215. https://doi.org/10.1016/S0065-2113(10)07005-7

Stevens, A., & Ramirez-Lopez, L. (2022). *An introduction to the prospectr package, R package vignette R package version 0.2.6*.

Tang, Y., Jones, E., & Minasny, B. (2020). Evaluating low-cost portable near infrared sensors for rapid analysis of soils from south eastern Australia. *Geoderma Regional*, *20*, e00240. https://doi.org/10.1016/j.geodrs.2019.e00240

Thomas, F., Petzold, R., Becker, C., & Werban, U. (2021). Application of low-cost mems spectrometers for forest topsoil properties prediction. *Sensors*, *21*, 1–21. https://doi.org/10.3390/s21113927

Viscarra Rossel, R. A., & Behrens, T. (2010). Using data mining to model and interpret soil diffuse reflectance spectra. *Geoderma*, *158*, 46–54. https://doi.org/10.1016/j.geoderma.2009.12.025

Viscarra Rossel, R. A., Behrens, T., Ben-Dor, E., Chabrillat, S., Demattê, J. A. M., Ge, Y., Gomez, C., Guerrero, C., Peng, Y., Ramirez-Lopez, L., Shi, Z., Stenberg, B., Webster, R., Winowiecki, L., & Shen, Z. (2022). Diffuse reflectance spectroscopy for estimating soil properties: A technology for the 21st century. *European Journal of Soil Science*, *73*, 1–9. https://doi.org/10.1111/ejss.13271

Viscarra Rossel, R. A., Cattle, S. R., Ortega, A., & Fouad, Y. (2009). In situ measurements of soil colour, mineral composition and clay content by Vis-NIR spectroscopy. *Geoderma*, *150*, 253–266. https://doi.org/10.1016/j.geoderma.2009.01.025

Viscarra Rossel, R. A., Walvoort, D. J. J., McBratney, A. B., Janik, L. J., & Skjemstad, J. O. (2006). Visible, near infrared, mid infrared or combined diffuse reflectance spectroscopy for simultaneous assessment of various soil properties. *Geoderma*, *131*, 59–75. https://doi.org/10.1016/j.geoderma.2005.03.007

Wall, D., & Plunkett, M. (Eds.). (2016). *Major & Micro Nutrient Advice for Productive Agricultural Crops* (4th ed.). Teagasc Johnstown Castle.

Wickham, H., Averick, M., Bryan, J., Chang, W., McGowan, L., François, R., Grolemund, G., Hayes, A., Henry, L., Hester, J., Kuhn, M., Pedersen, T., Miller, E., Bache, S., Müller, K., Ooms, J., Robinson, D., Seidel, D., Spinu, V., ... Yutani, H. (2019). Welcome to the Tidyverse. *J. Open Source Softw.*, *4*, 1686. https://doi.org/10.21105/joss.01686

SUPPORTING INFORMATION

Additional supporting information can be found online in the Supporting Information section at the end of this article.

How to cite this article: Metzger, K., Liebisch, F., Herrera, J. M., Guillaume, T., Walder, F., & Bragazza, L. (2024). The use of visible and near-infrared spectroscopy for in-situ characterization of agricultural soil fertility: A proposition of best practice by comparing scanning positions and spectrometers. *Soil Use and Management*, *40*, e12952. https://doi.org/10.1111/sum.12952